

One-side forward-backward asymmetry at the LHC

You-kai Wang¹ *, Bo Xiao¹ †, and Shou-hua Zhu^{1,2} ‡

¹ *Institute of Theoretical Physics & State Key Laboratory of Nuclear Physics and Technology,
Peking University, Beijing 100871, China*

² *Center for High Energy Physics, Peking University, Beijing 100871, China*

(Dated: October 30, 2018)

Forward-backward asymmetry A_{FB} is an essential observable to study the nature of coupling in the standard model and physics beyond the standard model, as shown at LEP and Tevatron. As a proton-proton collider, the LHC does not have the preferred direction contrary to her counterpart, namely, LEP and Tevatron. Therefore A_{FB} is not applicable at the LHC. However for the proton the momentum of valence quark is usually larger than that of the sea quark. Utilizing this feature we have defined a so-called one-side forward-backward asymmetry A_{OFB} for the top quark pair production at LHC in the previous work. In this paper we extend our studies to the charged leptons and bottom quarks as the final states. Our numerical results show that at the LHC A_{OFB} can be utilized to study the nature of the couplings once enough events are collected.

PACS numbers: 14.60.-z, 14.65.Fy, 12.15.-y, 12.38.Bx

I. INTRODUCTION

At high energy colliders discovering a new particle is not enough, one of the most important subsequent tasks is how to pin down its properties, for example, spin, nature of the coupling, and so on. Based on this information the internal quantum structure can be scrutinized and the possible subtle deviation may be found. In practice once enough data sample is collected, the forward-backward asymmetry (A_{FB}) for a specific final state can be measured and compared with theoretical prediction.

* E-mail:wangyk@pku.edu.cn

† E-mail:homenature@pku.edu.cn

‡ E-mail:shzhu@pku.edu.cn

A_{FB} , or sometimes called the charge asymmetry if CP conservation is assumed, is an interesting experimental observable. The primary definition of the A_{FB} is

$$A_{\text{FB}} \equiv \frac{N(\cos \theta > 0) - N(\cos \theta < 0)}{N(\cos \theta > 0) + N(\cos \theta < 0)}, \quad (1)$$

where θ is the polar angle between the final state particle and the beam line. The polar angle in Eq.(1) can be defined in different frames, such as Collins-Soper frame for the lepton pair production in the Drell-Yan processes, lab frame, and $t\bar{t}$ rest frame for top pair production process at Tevatron. In the $t\bar{t}$ rest frame, Eq.(1) can be transformed as

$$A_{\text{FB}} = \frac{\sigma(\Delta Y > 0) - \sigma(\Delta Y < 0)}{\sigma(\Delta Y > 0) + \sigma(\Delta Y < 0)}, \quad (2)$$

where $\Delta Y \equiv Y_t - Y_{\bar{t}}$ is the difference of rapidity of the top and antitop quark, which is invariant under $t\bar{t}$ or $p\bar{p}$ rest frame. Here the use of anti-top quark information implies that CP conservation of the top and antitop quark is assumed.

In some sense A_{FB} is a measure to study the angular distributions of the specific final particle. The distribution is determined by the nature of the couplings among the initial and final particles with the intermediate particle in a certain theory. Currently the successful theory which can describe the data is the standard model (SM). There are good reasons to expect physics beyond the SM (BSM), which usually predict new particles and/or new couplings. Such new particles and/or couplings can be firstly detected via A_{FB} measurements, namely, the deviation from the SM prediction. Therefore A_{FB} is a useful tool to test SM and even to discover BSM.

Up to now, A_{FB} for many final particles, e.g., charged leptons, bottom quark, and top quark have been measured at different colliders, say SLD, LEP and Tevatron. Generally speaking, the measurements are in excellent agreement with SM predictions. However there are some anomaly for the bottom quark at LEP and for the top quark at Tevatron. The measurements and theoretical predictions are listed in Table I.

Both A_{FB} measurements have a deviation about 2σ from SM predictions. It is obvious that only less than 3σ deviation is inadequate to conclude the failure of the SM. However it is interesting to explore the implications of the deviations both in the SM and the BSM [4–21]. The present experimental results still have too large uncertainties to make a clear judgement. So the cross-check of these measurements in the more powerful collider are extremely necessary.

TABLE I: Measurements and theoretical predictions (in bracket) of A_{FB} for bottom and top quark. Here $p\bar{p}$ and $t\bar{t}$ represent measurements in the lab and the center-of-mass frame of the top quark pair respectively.

	Bottom	Top
LEP	0.0992 ± 0.0016 (0.10324 ± 0.00088) [1]	...
		CDF $t\bar{t}$ $0.158 \pm 0.072 \pm 0.017$ (0.058 ± 0.009) [2]
Tevatron	...	CDF $p\bar{p}$ $0.150 \pm 0.050 \pm 0.024$ (0.038 ± 0.006) [2]
		D0 $t\bar{t}$ $0.08 \pm 0.04 \pm 0.01$ ($1_{-1}^{+2}\%$) [3]

The large hadron collider (LHC) is the most hopeful machine to make this cross-check and even discovery, because it has the larger production rate and most importantly, the more powerful reconstruction capacity of both the bottom and top quark. Unfortunately, unlike the e^+e^- collider, LEP, or $p\bar{p}$ collider, Tevatron, the pp collider, LHC, does not have preferred direction in the laboratory frame. The definition of A_{FB} in Eqs.(1) and (2) are not applicable here. Forward-backward asymmetry at pp collider has already been discussed in the literature[22–27]. A_{FB} in these papers are mostly used for exploiting a possible massive Z' boson. For example, A_{FB} can be defined as[26, 27]

$$A_{\text{FB}} = \frac{\int [F(y) - B(y)] dy}{\int [F(y) + B(y)] dy} \quad (3)$$

where $F(y)$ is the number of forward events with pseudorapidity $|\eta_f| > |\eta_{\bar{f}}|$ and $B(y)$ is the number of backward events with pseudorapidity $|\eta_f| < |\eta_{\bar{f}}|$ for a given Z' rapidity, y . In a previous paper, we proposed a new definition of forward-backward asymmetry, namely, the one-side forward-backward asymmetry A_{OFB} , to study the forward-backward asymmetry at the LHC[28]. The basic idea is that valence quark momentum is averagely larger than that of sea quark in the proton. Once the z direction momentum of the final states is required to be larger than a specific value, the partonic forward-backward asymmetry will be kept.

A_{OFB} is defined as

$$A_{\text{OFB}} = \frac{F_- + B_-}{F_+ + B_+} \equiv \frac{\sigma^A}{\sigma} \quad (4)$$

with

$$F_{\pm} = (\sigma(\Delta Y > 0) \pm \sigma(\Delta Y < 0))|_{P_{f+f-}^z > P_{\text{cut}}^z, M_{f+f-} > M_{\text{cut}}} \quad (5)$$

$$B_{\pm} = (\sigma(\Delta Y < 0) \pm \sigma(\Delta Y > 0))|_{P_{f^+f^-}^z < -P_{\text{cut}}^z, M_{f^+f^-} > M_{\text{cut}}} \quad (6)$$

where $P_{f^+f^-}^z$ is the final particle pair's z direction momentum and $M_{f^+f^-}$ is the invariant mass of the final particle pair.

By adopting some kinematic cuts, especially cuts on $P_{f^+f^-}^z$, the forward-backward asymmetry generated at the partonic level can be kept even after the convolution with parton distribution functions. The A_{OFB} can be an efficient tool in investigating the forward-backward asymmetry at the LHC. In principle, all the forward backward asymmetry measured in the left right asymmetric beam collides, eg., e^+e^- or $p\bar{p}$, can now be cross-checked at the left right symmetric pp beam collider, LHC. In this paper, we will extend our previous study to various final state cases[28].

As shown in Eq.(4), the precise momentum measurement at z direction is essential for A_{OFB} . At the LHC, the momentum of charged leptons are the most precisely measured quantities. Thus it is quite natural to study first the A_{OFB} for charged leptons at the LHC. In the SM, the charged lepton pair can be generated via s channel Z and/or γ^* electroweak (EW) diagrams, and these tree-level diagrams can contribute to A_{OFB} because the couplings of left- and right-handed fermions with gauge boson Z are different. At the LHC, besides the s channel Z and/or γ^* induced EW diagrams, bottom quarks are also produced via the strong interaction. The contributions to A_{OFB}^b in QCD starts from the next-to-leading order, namely, at $\mathcal{O}(\alpha_S^3)$ [29, 30]. The situation is similar to that of top quark pair production [28]. Away from Z -pole, the EW contributions to A_{OFB}^b is much less than that of QCD ones. In order to study A_{OFB}^b arising from the EW source, we have to select events around the Z -pole.

The paper is organized as following. In Sec. II, the charged lepton one-side forward backward asymmetry A_{OFB}^ℓ at the LHC is calculated. As the charged lepton momentum can be precisely measured, A_{OFB}^ℓ can be a test ground of the newly proposed one-side forward-backward asymmetry. In Sec. III, A_{OFB}^b is calculated at the NLO in QCD. In section IV, A_{OFB}^b is calculated in the vicinity of the Z pole in order to study the EW origin of forward-backward asymmetry. Section V contains our conclusions and discussions.

II. CHARGED LEPTON ONE-SIDE FORWARD-BACKWARD ASYMMETRY

$$A_{\text{OFB}}^{\ell}$$

At the LHC, the main production mechanisms of the charged leptons (electron/muon/tau) at partonic level are $q\bar{q} \rightarrow Z/\gamma^* \rightarrow l^+l^-$, similar to those at LEP and Tevatron. Because the couplings among Z boson and left- or right-handed fermions are different, even at leading order $\mathcal{O}(\alpha^2)$, forward-backward asymmetry is non-zero¹. The measurements of A_{FB}^{ℓ} (cf. Eq. 1) at LEP and Tevatron are in good agreement with the SM predictions. At the LHC there is no preferred direction in lab frame. The one-side forward-backward asymmetry for l^+l^- production process is defined as Eq.(4), where

$$F_{\pm} = (\sigma(\Delta Y > 0) \pm \sigma(\Delta Y < 0))|_{P_{l^+l^-}^z > P_{\text{cut}}^z} \quad (7)$$

$$B_{\pm} = (\sigma(\Delta Y < 0) \pm \sigma(\Delta Y > 0))|_{P_{l^+l^-}^z < -P_{\text{cut}}^z}. \quad (8)$$

Here $\Delta Y = Y_{l^+} - Y_{l^-}$ is the difference of rapidity of the charged leptons, which is invariant along the boost in beam directions. $P_{l^+l^-}^z$ is the z direction momentum of the lepton pair in the laboratory frame.

At the pp collider LHC, for the subprocess $q\bar{q} \rightarrow l^+l^-$, the momentum of the valence quark q is usually larger than that of the sea quark \bar{q} . If taking the momentum of q as the positive z direction, we will get $P_{l^+l^-}^z > 0$. However there is the possibility that momentum of valence quark is less than that of sea quark. In this case, $P_{l^+l^-}^z < 0$. This will induce the opposite contribution to asymmetric cross section. Moreover, the valence quark can symmetrically come from the other proton. The usual A_{FB} is strictly equal to zero. The asymmetric cross section of the partonic processes can survive only if we just observe one-side l^+l^- events, for example $P_{l^+l^-}^z > 0$ or $P_{l^+l^-}^z > P_{\text{cut}}^z$. The usual forward cross section $\sigma(\Delta Y > 0)$ and backward cross section $\sigma(\Delta Y < 0)$ can be calculated after imposing the $P_{l^+l^-}^z$ cut. So the forward-backward asymmetry in this side is F_-/F_+ . If we evaluate the opposite side events, namely, $P_{l^+l^-}^z < -P_{\text{cut}}^z$, the forward-backward asymmetry in this side is B_-/B_+ . At the LHC the consistence between these two forward-backward asymmetries can be checked. Moreover if we define A_{OFB} in Eq.(4), the statistics will be doubled. Besides keeping the forward-backward asymmetry at partonic level, P_{cut}^z has other advantages for example increasing the significance to observe the forward-backward asymmetry.

¹ For $e^+e^- \rightarrow e^+e^-$ the $A_{\text{FB}} \neq 0$ arises also from the interference between s- and t-channel QED diagrams.

In our calculations here, F_{\pm} and B_{\pm} are calculated at the leading order $\mathcal{O}(\alpha^2)$. Because of the small mass compared with the collider beam energy, three charged leptons will have similar signatures although they will be measured (reconstructed) by different methods. Limited by the coverage of the real detector, the charged lepton is required to satisfy $|\eta| < 2.4$ [31]. In massless limit, $\eta = Y$.

Figures 1 and 2 show the differential spectrum of the asymmetric cross section σ^A , total cross section σ , A_{OFB} as a function of the lepton pair invariant mass $M_{e^+e^-}$ (taking electron as the example), and the significance $\text{sig} = \sqrt{\mathcal{L}}\sigma^A/\sqrt{\sigma}$ (with $\mathcal{L} = 10fb^{-1}$) as a function of P_{cut}^z at the LHC for $\sqrt{s} = 7$ TeV and 14 TeV respectively. No η cuts are applied for the left column plots, and $|\eta| < 2.4$ is applied for the right column plots. The significance plots are used to select the optimal P_{cut}^z . In these plots we take the typical value $M_{e^+e^-} = 100.5\text{GeV}$ as an example. The optimal P_{cut}^z are not sensitive to $M_{e^+e^-}$. Thus, we take $P_{\text{cut}}^z = 150\text{GeV}$ in the left upper three plots and $P_{\text{cut}}^z = 50\text{GeV}$ in the right upper three plots. From the curves with and without η cut we can see that the asymmetric cross section is sensitive to η . This behavior indicates that asymmetric cross section is mostly located in large η region due to the large boost along the longitudinal direction. From figures we can also see clearly the resonance around Z in $d\sigma/dM_{e^+e^-}$ and $d\sigma^A/dM_{e^+e^-}$. Moreover, the A_{OFB} varies with $M_{e^+e^-}$ and the distribution is similar to that of usual A_{FB} at e^+e^- and $p\bar{p}$ colliders. The reason is simply because both A_{OFB} and A_{FB} arise mainly from the same subprocesses $u\bar{u} \rightarrow e^+e^-$ and $d\bar{d} \rightarrow e^+e^-$.

For our purpose we only study the A_{OFB} at leading order, namely, at $\mathcal{O}(\alpha^2)$. In practice [32] higher-order effects must be included. Such higher-order effects, especially the contributions from the high P_T l^+l^- events which arise from the extra hard photon radiation, can be treated by adopting Collins-Soper frame [32–34]. The advantage of adopting the Collins-Soper frame is that A_{FB} is free from the impact of the $2 \rightarrow 3$ process with initial γ radiation which will cause a nonzero P_T of the lepton pair. A_{OFB} can also be extended to Collins-Soper frame with extra cut on z-direction momentum of lepton pair. We will study this issue in detail elsewhere.

One-side forward-backward asymmetry can be tested in the charged lepton production processes. Theoretically A_{OFB} can also be utilized to study the more complicated bottom quark production at the LHC, though in practice the channel is not as clean as that of charged leptons.

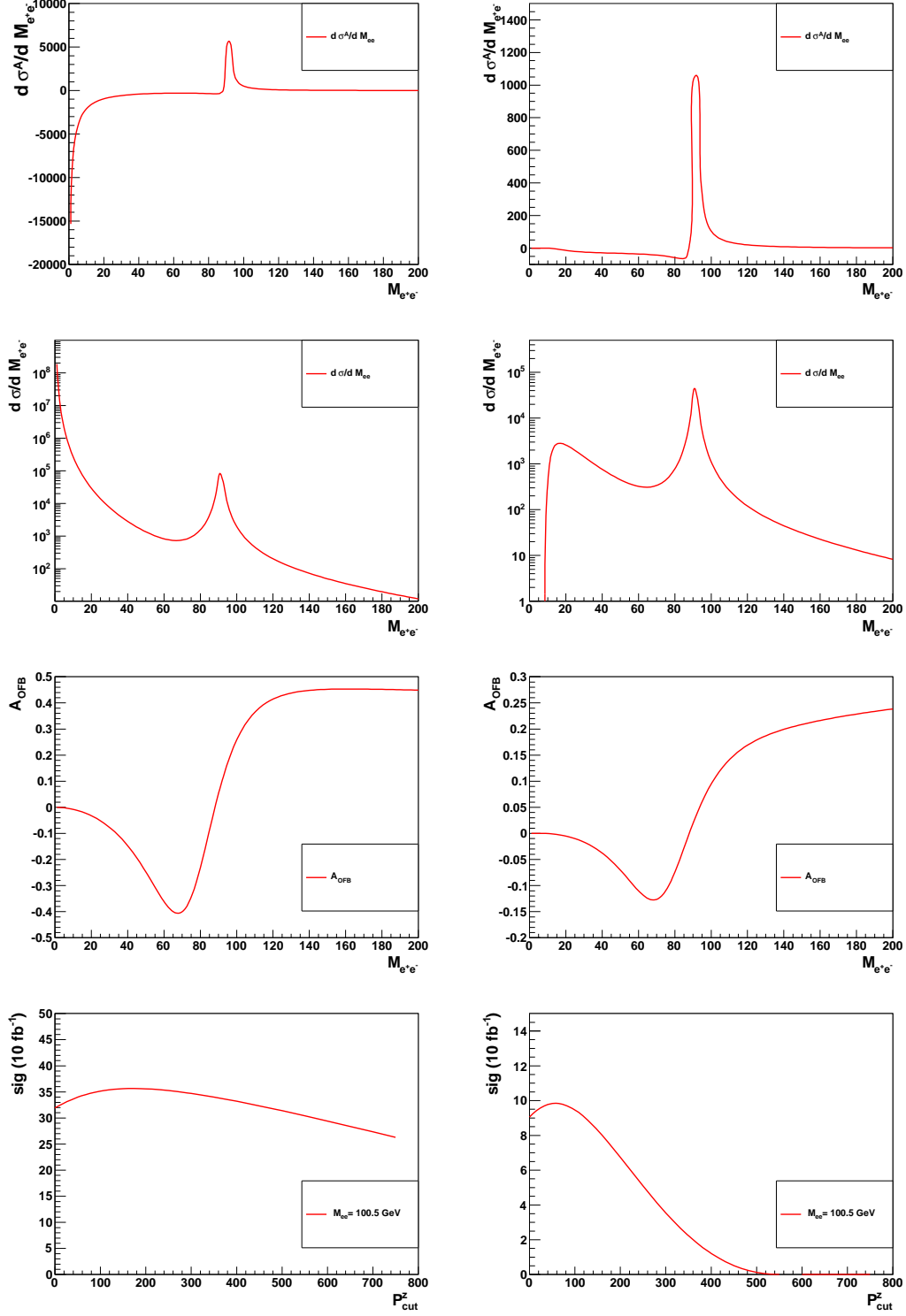


FIG. 1: $d\sigma^A/dM_{e^+e^-}$, $d\sigma/dM_{e^+e^-}$, A_{OFB} as a function of $M_{e^+e^-}$ and sig as a function of P_{cut}^z at the LHC for $\sqrt{s} = 7$ TeV. The left plots have no η cut, and the right plots have $|\eta| < 2.4$ cut. Optimal P_{cut}^z are determined by the sig plots. The left upper three plots have $P_{\text{cut}}^z = 150\text{GeV}$ and the right upper three plots have $P_{\text{cut}}^z = 50\text{GeV}$.

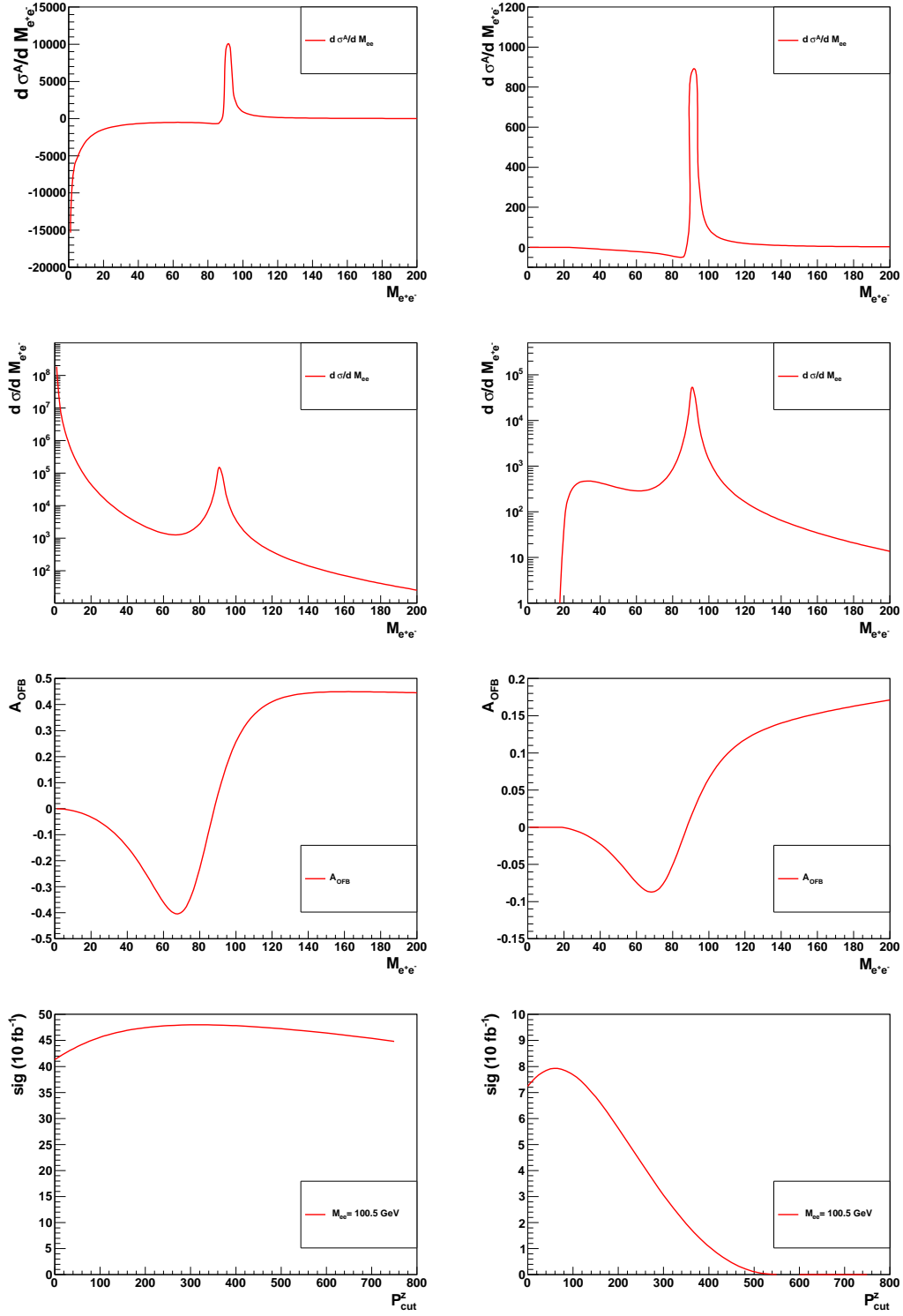


FIG. 2: Same as Fig. 1 except $\sqrt{s} = 14$ TeV. Optimal $P_{cut}^z = 300$ GeV for left upper three plots and optimal $P_{cut}^z = 100$ GeV for right upper three plots.

III. BOTTOM QUARK ONE-SIDE FORWARD-BACKWARD ASYMMETRY

A_{OFB}^b IN QCD

Unlike the top quark, the bottom quark life time is longer than the hadronization scale, which means bottom quark will appear as b jet in the detector. For simplicity in our analysis, we treat the b quark as b jet in the calculation.

As mentioned above, at the LHC, the bottom quark forward backward asymmetry arises from two sources, namely, the QCD and EW processes. The dominant bottom quark production processes are $gg(q\bar{q}) \rightarrow b\bar{b}$ via strong interaction. However at the leading order in QCD i.e. $\mathcal{O}(\alpha_s^2)$, the forward backward asymmetry is zero. The QCD induced asymmetric cross section starts from $O(\alpha_s^3)$. Same as top pair production, the contributions can be classified into three categories: (1) Interference among diagrams for the initial and final state radiation processes $q\bar{q} \rightarrow b\bar{b}g$; (2) Interference among the born diagrams and virtual box diagrams for the process $q\bar{q} \rightarrow b\bar{b}$; (3) Contribution from diagrams of the real processes $gg \rightarrow b\bar{b}q$. The calculation has been carried out in Ref. [29, 30]. For the EW interaction contribution, the leading contribution comes from the born cross section $q\bar{q} \rightarrow b\bar{b}$ via a Z and/or γ^* boson, similar with the case of charged lepton. At the LHC the EW contribution is mostly from the vicinity of the Z pole, while the QCD contribution extends in the wider energy regime. Moreover except at Z pole the QCD contribution is much larger than that of the EW one. In this section we will focus on the QCD contribution to A_{OFB}^b .

At the Tevatron the theoretical calculation of heavy quark forward backward asymmetry arising from the QCD contributions has been studied in previous literature [29, 30]. Even at the LHC, the so-called central charge asymmetry A_C has been constructed to study the forward backward asymmetry of the top quark [29, 30, 35–38]. Some comparison have been made between the central charge asymmetry and the one-side forward backward asymmetry in Ref. [28]. At the LHC A_{OFB} is much larger than A_C because P_{cut}^z can suppress the huge symmetric gg fusion efficiently.

One-side forward-backward asymmetry for b quark at the LHC can be defined in the pp rest frame as in Eq. 4,

$$F_{\pm} = (\sigma(\Delta Y > 0) \pm \sigma(\Delta Y < 0))|_{P_{bb}^z > P_{\text{cut}}^z, M_{b\bar{b}} > M_{\text{cut}}} \quad (9)$$

$$B_{\pm} = (\sigma(\Delta Y < 0) \pm \sigma(\Delta Y > 0))|_{P_{bb}^z < -P_{\text{cut}}^z, M_{b\bar{b}} > M_{\text{cut}}} \quad (10)$$

Here we only consider QCD contributions and ignore the electroweak contributions. The purpose to apply constraints on $P_{t\bar{t}}^z$ and $M_{t\bar{t}}$ is to suppress the symmetric $gg \rightarrow t\bar{t}$ events, which will be illustrated in the following figures.

To measure A_{OFB} at the LHC, the charge of the b jet should be identified to distinguish the bottom or anti-bottom jet. So one bottom/antibottom quark is required to decay into a charged lepton, and the other antibottom/bottom can decay hadronically. For the b tagging, there are two selecting criteria [39]: $P_T > 40\text{GeV}$ and $|\eta| < 1.5$ without second vertex reconstruction, and $P_T > 10\text{ GeV}$ and $|\eta| < 2.4$ with second vertex reconstruction. We find that our signal b jets locate mostly in large η regions due to the high longitudinal boost. So we take the second cut criteria in the following analysis.

Note that the definition in Eq.(4) is based on the CMS or ATLAS detector at the LHC. For the LHCb, one can take real ‘‘one-side’’ definition, namely

$$A_{\text{OFB}} = \frac{F_-}{F_+}. \quad (11)$$

In this case b tagging requirements should also be adjusted accordingly. The obvious difference is that there will be a lower bound on η , e.g. $2.0 < \eta < 5.5$ [40]. As most of $b\bar{b}$ events are boosted in the z -direction, LHCb has the unique advantage to collect more bottom events to reach higher precision measurement of forward-backward asymmetry.

Figure 3 shows the asymmetric cross section σ^A , symmetric cross section σ , A_{OFB} and significance sig (with $\mathcal{L} = \infty/\text{fb}^{-\infty}$) as a function of P_{cut}^z without and with b jet cut for $\sqrt{s} = 7\text{ TeV}$. From the left column plots, we see that both σ^A and σ drop with the increase of P_{cut}^z . σ decreases even faster so A_{OFB} rises with the increase of P_{cut}^z . This is due to two reasons. First, as mentioned in above sections, A_{OFB} will be polluted by the negative contributions to asymmetric cross section in the case that the sea quark’s momentum is larger than the valence quark’s momentum. These events locates mostly in small $P_{b\bar{b}}^z$ region. A larger cut of $P_{b\bar{b}}^z$ can increase the portion of positive sign asymmetric cross section. Second, due to the properties of the parton distribution function, the symmetric $gg \rightarrow b\bar{b}$ events are mostly distributed in the small $P_{b\bar{b}}^z$ region and the asymmetric events are likely to be highly boosted along the z direction. The P_{cut}^z can remove more symmetric backgrounds.

The right column plots indicate that b jet cut can change the above distributions significantly. Most of the events are lost. Low $M_{b\bar{b}}$ events are more sensitive to b jet cuts than the large $M_{b\bar{b}}$ events, which indicates that they tends to have lager η and small P_T . The σ^A

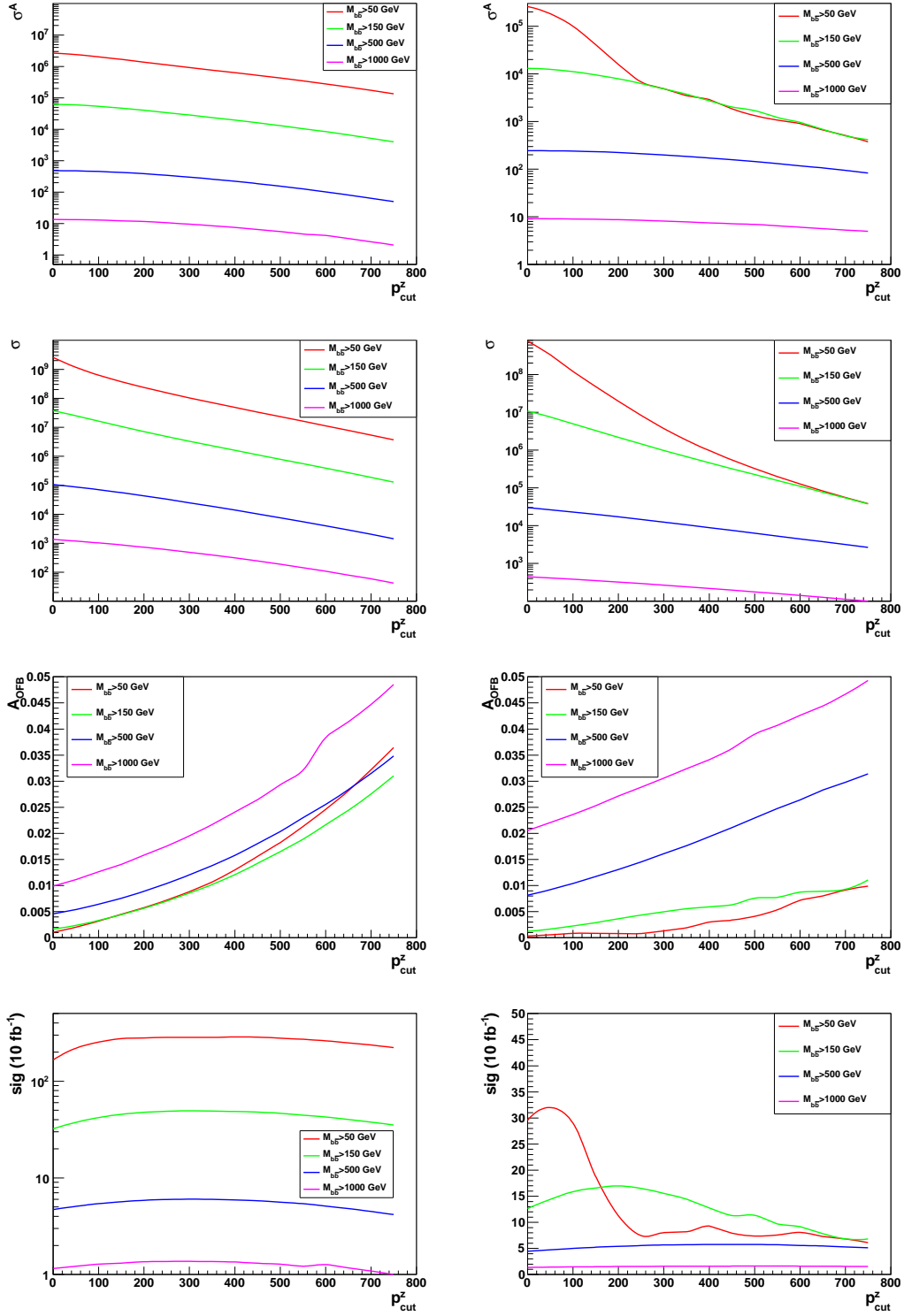


FIG. 3: σ^A , σ , A_{OFB} , and sig as a function of P_{bb}^z for $\sqrt{s} = 7 \text{ TeV}$. For the right (left) column plots b jet cuts are (not) applied.

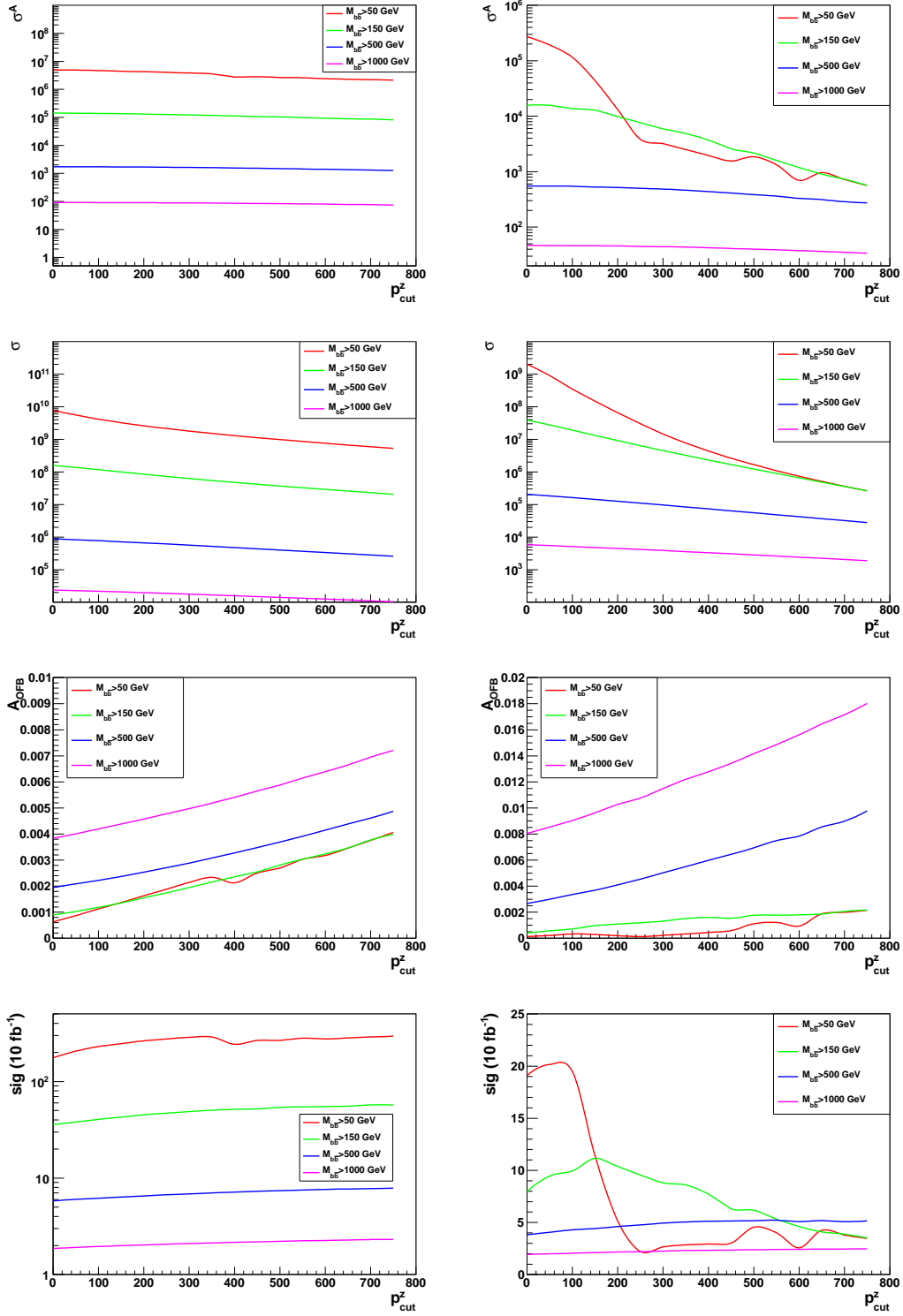


FIG. 4: Same as Fig. 3 except $\sqrt{s} = 14$ TeV.

plot shows that asymmetric events with $50\text{GeV} < M_{b\bar{b}} < 150\text{GeV}$ and $P_{b\bar{b}}^z > 250\text{GeV}$ are completely removed by b jet cut. Generally speaking, b jet cut is a very strong constraint on the forward-backward asymmetry measurements at the LHC. Because of the high energy at the LHC, most of the highly longitudinal boosted b quark are difficult to record in the detector. The significance can drop greatly in the real experimental environment. The situation becomes even harder for $\sqrt{s} = 14$ TeV as shown in Fig.4. Because of the even larger longitudinal boosts, precision measurements require higher integrated luminosity for $\sqrt{s} = 14$ TeV.

As mentioned above, forward backward asymmetry of the bottom quark has been measured at the LEP near the Z pole. As an e^+e^- collider, LEP's measurement can only show the EW contribution to the asymmetric cross section of the b quark. Although Tevatron has already measured the top quark forward backward asymmetry, the forward backward asymmetry of the bottom quark at the hadron collider, which are mainly contributed from the QCD interference diagrams, is still not investigated yet. According to the above studies, it is still hopeful that this QCD induced asymmetric signature can be seen at the LHC detectors. Previous measurements show the top quark forward backward asymmetry has about 2 standard deviation from the QCD prediction [2, 3]. Many new physics beyond the SM have been studied to explain this novel signature [6–19]. It will be very interesting to see whether the bottom quark, which belongs to the third generation, has similar deviation as the top quark.

IV. BOTTOM QUARK ONE-SIDE FORWARD-BACKWARD ASYMMETRY

A_{OFB}^b AROUND Z-POLE

In Sec. III we investigated how to study QCD induced A_{OFB}^b . In a wide energy regime, electroweak contribution to the forward-backward asymmetry is much less than the QCD contribution. By requiring the final $b\bar{b}$ invariant mass near the Z -pole, most of QCD contribution to the asymmetric cross section can be suppressed and the remaining QCD and the electro-weak induced asymmetric cross section can be comparable. So, the LHC can also explore the electroweak induced asymmetric cross section for the bottom quark. Such measurements are the nearest hope to do the cross-check to the corresponding measurements at the LEP.

The one-side forward-backward asymmetry near the Z pole can be defined as in Eq. 4 with

$$F_{\pm} = (\sigma(\Delta Y > 0) \pm \sigma(\Delta Y < 0))|_{P_{bb}^z > P_{\text{cut}}^z, m_Z - \delta E/2 < M_{bb} < m_Z + \delta E/2} \quad (12)$$

$$B_{\pm} = (\sigma(\Delta Y < 0) \pm \sigma(\Delta Y > 0))|_{P_{bb}^z < -P_{\text{cut}}^z, m_Z - \delta E/2 < M_{bb} < m_Z + \delta E/2} \quad (13)$$

in which δE is the energy window near the Z pole. Both EW and QCD contribution should be included in the calculation. For the EW processes, we calculate the contribution at the leading order $\mathcal{O}(\alpha^2)$. For the QCD processes, we include the NLO QCD contribution in the numerator and LO QCD ones in the denominator [28].

Figure 5 shows σ^A , σ , A_{OFB} and sig of the bottom quark as a function of P_{cut}^z at the LHC with $\sqrt{s} = 7$ TeV with and without b jet cut. Without b -jet cuts, A_{OFB} will rise with the increase of P_{bb}^z , and the behavior is the same with the case in section III. Cuts on b jet will greatly change the distribution of A_{OFB} and sig . The figure indicates that large P_{bb}^z events are highly boosted in the z -direction, which means they have small P_T and large η . All σ^A events with $P_{bb}^z > 450\text{GeV}$ will be cut off by requiring the b jet $|\eta| < 2.4$ and $P_T > 10\text{GeV}$. Theoretically, A_{OFB} can be very large in high P_{bb}^z region. However, limited by the coverage of the real detector, identifying these events is quite challenging.

In Fig. 5, we can see that σ is approximately proportion to δE while σ^A raise with the increase of δE more slowly. This is because σ mainly comes from QCD contribution, which distributes evenly around the Z -pole, while σ_A mainly comes from EW contribution, which distributes sharply around Z -pole. So A_{OFB} decrease with the increase of δE . A_{OFB} is harder to be measured for $\sqrt{s} = 14\text{TeV}$ due to the larger longitudinal boost as shown in Fig. 6.

Figure 7 show the differential σ^A , σ and A_{OFB} as a function of M_{bb} at the LHC with $\sqrt{s} = 7$ TeV and 14 TeV respectively. Here the b jet cut $|\eta| < 2.4$ and $P_T > 10\text{GeV}$ are applied. $P_{bb}^z = 150$ GeV is the optimal cut which can be seen in the right lower sig plot in Figs. 5 and 6. From Fig. 7 we can see that σ^A is dominated by the contribution from EW processes, while the total cross section σ arises mostly from QCD processes.

In order to do the cross-check with the measurements at the LEP, the clear understanding of the QCD contributions is necessary. This can be carried out by the measurements in a wide $b\bar{b}$ energy interval discussed in Sec. III in which A_{OFB} is dominated by the QCD contribution, or in a small M_{bb} region far away from the Z -pole.

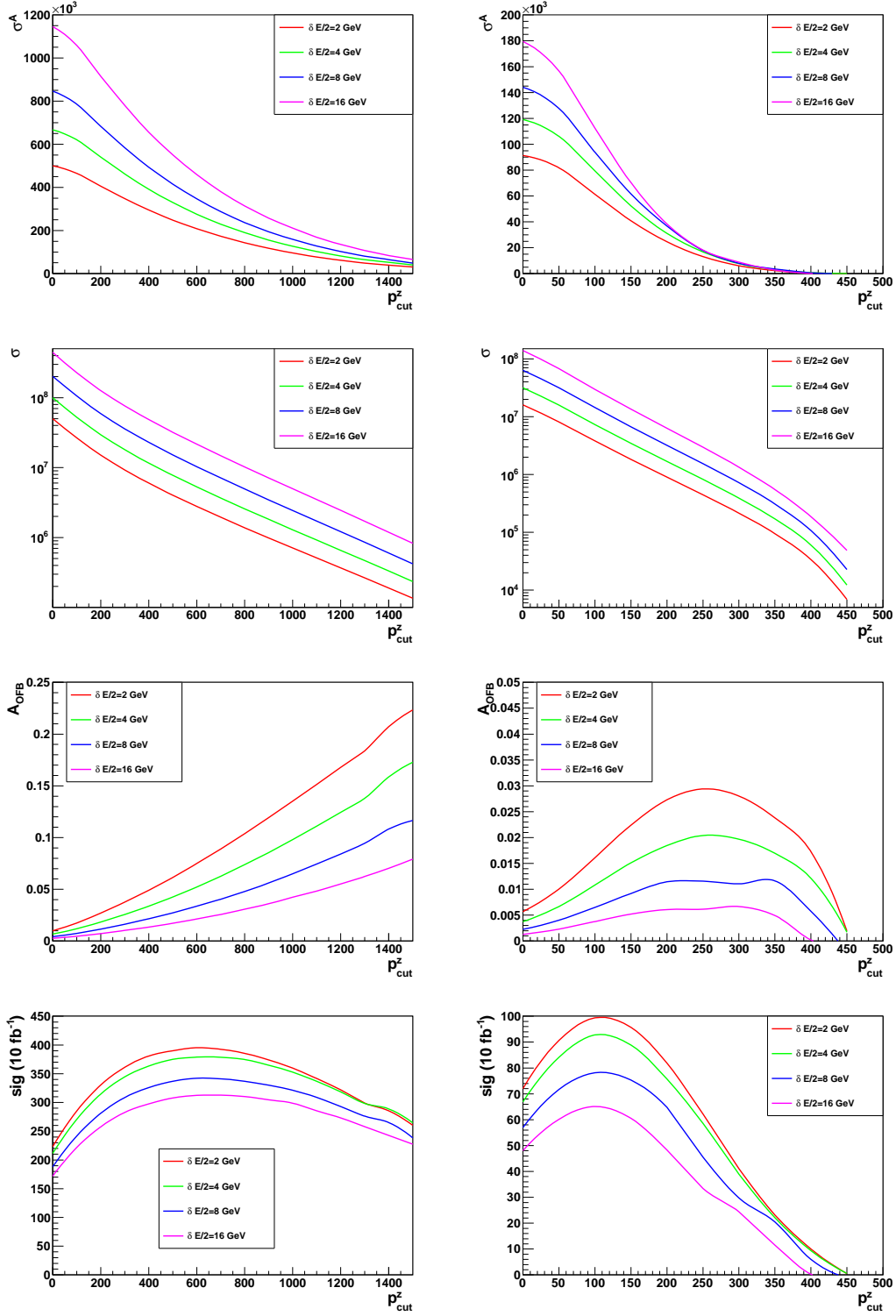


FIG. 5: σ^A , σ , A_{OFB} and sig as a function of P_{cut}^z at LHC with $\sqrt{s} = 7$ TeV. For the right (left) column plots b jet cuts are (not) applied.

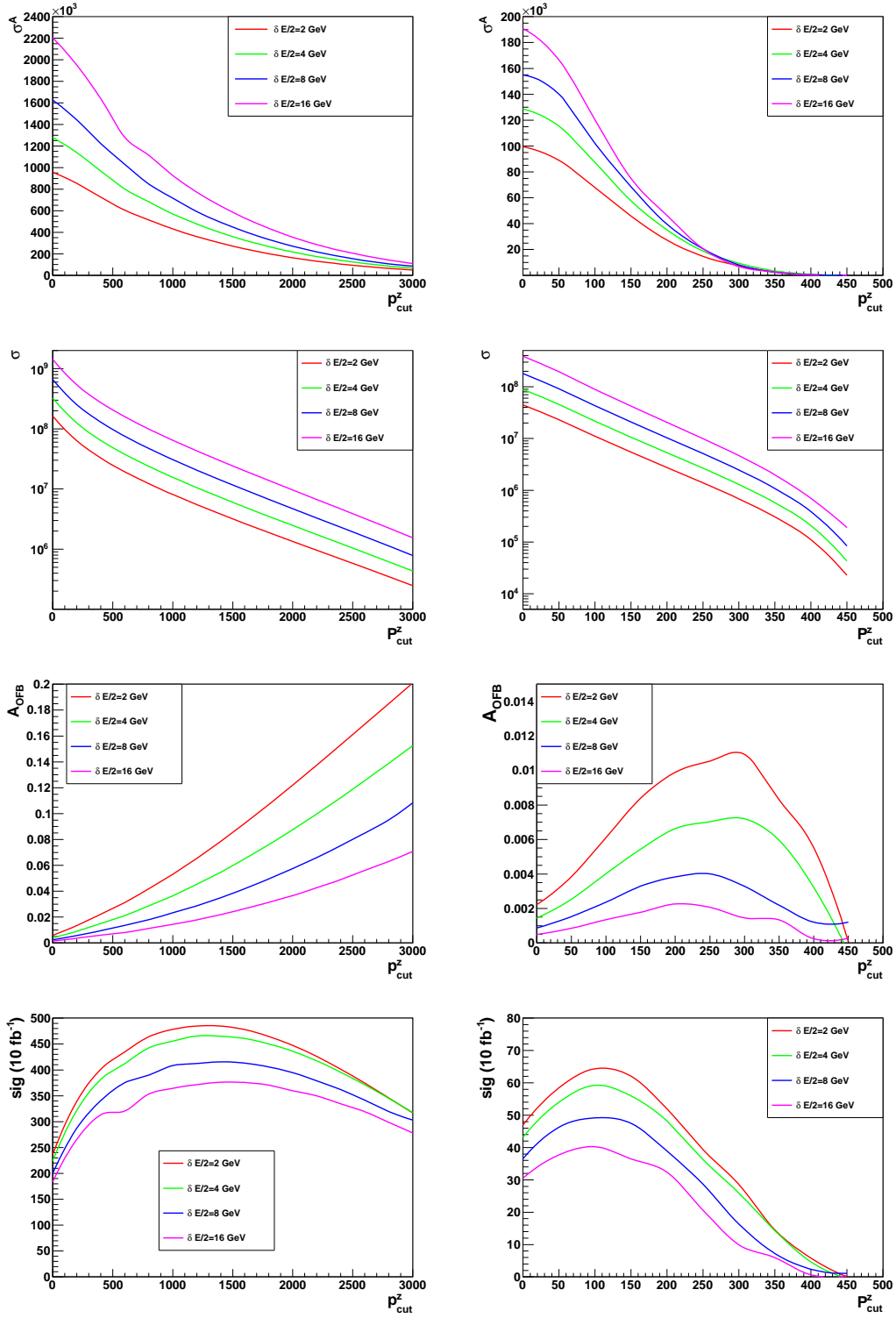


FIG. 6: Same as Fig. 5 except $\sqrt{s} = 14$ TeV.

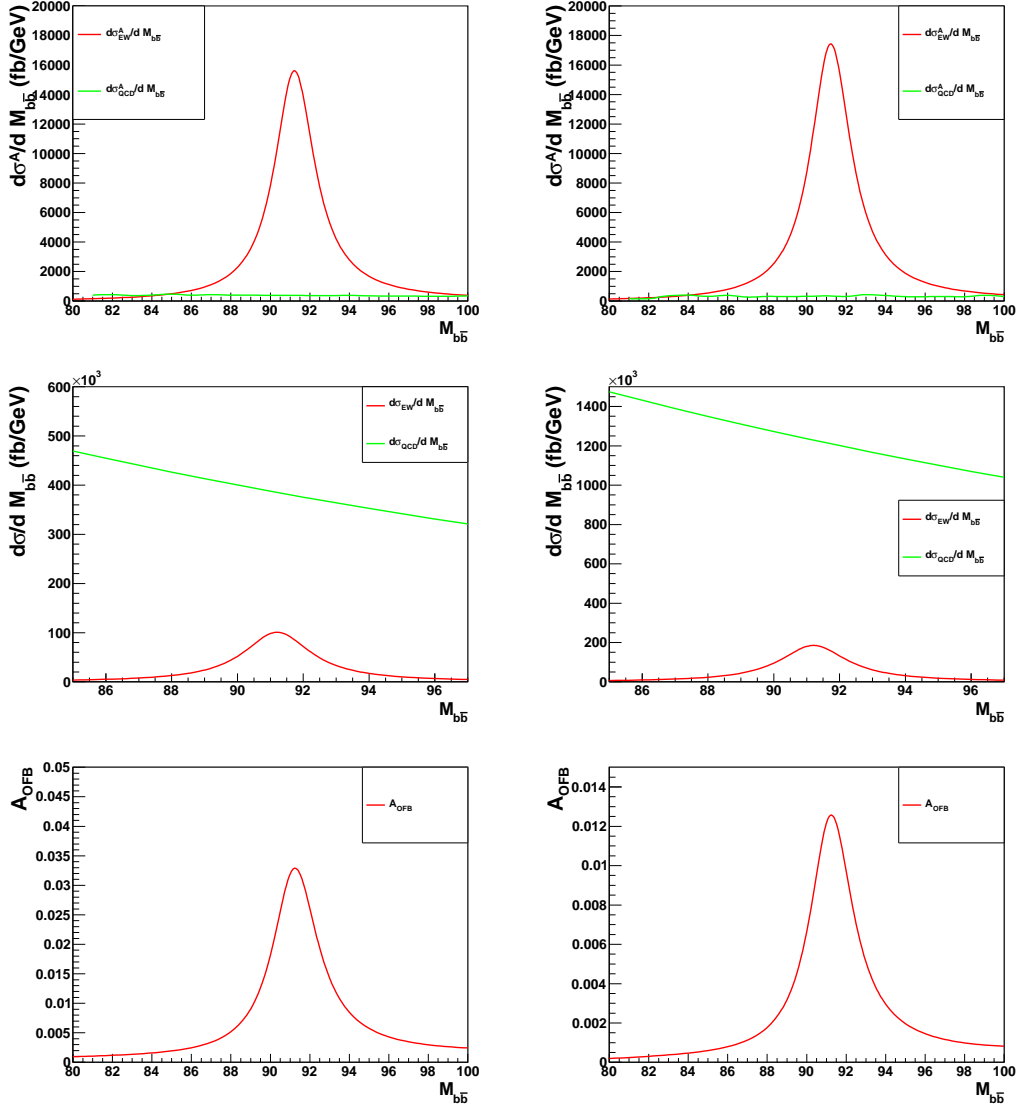


FIG. 7: Differential distributions of σ^A , σ and A_{OFB} with $\sqrt{s} = 7$ TeV (left column) and $\sqrt{s} = 14$ TeV (right column). Here b jet cut is applied. $P_{bb}^z = 150$ GeV. Here A_{OFB} contains contribution from both EW and QCD.

It is quite interesting to estimate how much integrated luminosity is needed in order to achieve the similar precision of A_{FB}^b at the LEP. We only give a rough estimation here and a precise study needs complicated real detector simulation, which is beyond the current discussion. As a e^+e^- collider, A_{FB}^b arises mainly from EW interaction. However, A_{OFB}^b at the LHC have both EW and QCD contributions. Noticing that the EW and QCD contributions have different distribution shapes as shown in Fig. 7, the QCD induced asymmetric and symmetric events can be removed as a continuous background and pure EW induced asymmetry can be

defined as $A_{\text{EWOFB}}^b = N_{\text{EW}}^A/N_{\text{EW}}$. According to the error propagation formula, the statistical fluctuation of A_{EWOFB}^b can be expressed as $\sigma(A_{\text{EWOFB}}^b) = \sqrt{4N_{\text{EW}}^F N_{\text{EW}}^B / (N_{\text{EW}}^F + N_{\text{EW}}^B)^3}$, where $N_{\text{EW}}^F/N_{\text{EW}}^B$ are EW induced forward/backward events. For a comparable precision, it can be required that the statistical fluctuation of A_{EWOFB}^b at the LHC should be of the same order $O(0.001)$ as that of A_{FB}^b at the LEP. By taking the relative data in Fig. 7 into $\sigma(A_{\text{EWOFB}}^b)$, the effective luminosity is calculated to be $\epsilon\mathcal{L} = 9.8 \text{ fb}^{-1}$ for 7 TeV and $\epsilon\mathcal{L} = 5.0 \text{ fb}^{-1}$ for 14 TeV. Here ϵ is the b quark selecting efficiency.

V. CONCLUSIONS AND DISCUSSIONS

Forward backward asymmetry A_{FB} is a tool to study the nature of couplings, even the quantum structure in the SM and/or BSM. In the past measurements at the LEP and Tevatron, the deviations from the SM predictions have inspired extensive studies in the SM/BSM. However as the proton-proton collider, the LHC does not have the preferred direction contrary to her counterpart, namely LEP and Tevatron. By utilizing the property that the momentum of valence quark is usually larger than that of sea quark, the preferred direction at parton level can be kept. For the top pair production at LHC, we have proposed to apply cut on z direction momentum of the top quark pair in order to keep the forward backward asymmetry at partonic level, dubbed as one-side forward backward asymmetry A_{OFB} . In this paper we extend our studies to the charged leptons and bottom quarks as the final states. Our numerical results show that at the LHC A_{OFB} can be utilized to study the nature of the couplings once enough events are collected.

There are some points we should emphasize: (1) Once the preferred direction at the LHC can be defined, A_{OFB} for any precisely measured final state particle can be utilized as a tool to study the structure in the SM and/or BSM; (2) Our studies, especially on the QCD induced A_{OFB} , indicate that the validity of the observable A_{OFB} does not depend on whether the higher order effects is included or not; (3) The backgrounds to the specific final states are not included in our study, however in the realistic analysis this issue should be investigated in detail.

Acknowledgements: SHZ would thank Y. J. Mao and B. Zhu of CMS collaboration for the stimulating discussions. YKW would like to thank Xia Wan for the valuable discussions. This work was supported in part by the Natural Sciences Foundation of China (No.

10775001, No. 10635030, and No. 11075003).

- [1] ALEPH, DELPHI, L3, OPAL, SLD Collaborations, LEP Electroweak Working Group, SLD Electroweak and Heavy Flavour Groups, Phys. Rep. **427**, 257 (2006), hep-ex/0509008.
- [2] CDF Collaboration, CDFNote CDF/ANAL/TOP/PUBLIC/10224, 2010.
- [3] D0 Collaboration, D0Note 6062-CONF, 2010.
- [4] L. G. Almeida, G. F. Sterman, and W. Vogelsang, Phys. Rev. **D78**, 014008 (2008), arXiv:0805.1885.
- [5] V. Ahrens, A. Ferroglia, M. Neubert, B. D Pecjak and L. L. Yang, JHEP **09**, 097 (2010), arXiv:1003.5827.
- [6] P. H. Frampton, J. Shu, and K. Wang, Phys. Lett. **B683**, 294 (2010), arXiv:0911.2955.
- [7] J. Shu, T. M. P. Tait, and K. Wang, Phys. Rev. **D81**, 034012 (2010), arXiv:0911.3237.
- [8] R. S. Chivukula, E. H. Simmons, and C. P. Yuan, Phys. Rev. **D82**, 094009 (2010), arXiv:1007.0260.
- [9] S. Jung, H. Murayama, A. Pierce, and J. D. Wells, Phys. Rev. **D81**, 015004 (2010), arXiv:0907.4112.
- [10] K. Cheung, W.-Y. Keung, and T.-C. Yuan, Phys. Lett. **B682**, 287 (2009), arXiv:0908.2589.
- [11] Q.-H. Cao, D. McKeen, J. L. Rosner, G. Shaughnessy, and C. E. M. Wagner, Phys. Rev. **D81**, 114004 (2010), arXiv:1003.3461.
- [12] A. Djouadi, G. Moreau, F. Richard, and R. K. Singh, Phys. Rev. **D82**, 071702 (2010), arXiv:0906.0604.
- [13] D.-W. Jung, P. Ko, J. S. Lee, and S.-h. Nam, Phys. Lett. **B691**, 238 (2010), arXiv:0912.1105.
- [14] J. Cao, Z. Heng, L. Wu, and J. M. Yang, Phys. Rev. **D81**, 014016 (2010), arXiv:0912.1447.
- [15] V. Barger, W.-Y. Keung, and C.-T. Yu, Phys. Rev. **D81**, 113009 (2010), arXiv:1002.1048.
- [16] A. Arhrib, R. Benbrik, and C.-H. Chen, Phys. Rev. **D82**, 034034 (2010), arXiv:0911.4875.
- [17] B. Xiao, Y.-k. Wang, and S.-h. Zhu, Phys. Rev. **D82**, 034026 (2010), arXiv:1006.2510.
- [18] M. Bauer, F. Goertz, U. Haisch, T. Pfoh, and S. Westhoff, J. High Energy Phys. **11** (2010) 039, arXiv:1008.0742.
- [19] B. Xiao, Y.-k. Wang, and S.-h. Zhu, arXiv:1011.0152.
- [20] I. Dorsner, S. Fajfer, J. F. Kamenik and N. Kosnik, Phys. Rev. **D81**, 055009 (2010),

arXiv:0912.0972.

- [21] C.-H. Chen, G. Cvetič and C. S. Kim, Phys. Lett. B694: 393-397, 2011 arXiv:1009.4165.
- [22] P. Langacker, R. W. Robinett, and J. L. Rosner, Phys. Rev. **D30**, 1470 (1984).
- [23] M. Dittmar, Phys. Rev. **D55**, 161 (1997), hep-ex/9606002.
- [24] F. Petriello and S. Quackenbush, Phys. Rev. **D77**, 115004 (2008), arXiv:0801.4389.
- [25] Y. Li, F. Petriello, and S. Quackenbush, Phys. Rev. **D80**, 055018 (2009), arXiv:0906.4132.
- [26] R. Diener, S. Godfrey, and T. A. W. Martin, Phys. Rev. **D80**, 075014 (2009), arXiv:0909.2022.
- [27] R. Diener, S. Godfrey, and T. A. W. Martin, (2010), arXiv:1006.2845.
- [28] Y.-k. Wang, B. Xiao, and S.-h. Zhu, Phys. Rev. **D82**, 094011 (2010), arXiv:1008.2685.
- [29] J. H. Kuhn and G. Rodrigo, Phys. Rev. Lett. **81**, 49 (1998), hep-ph/9802268.
- [30] J. H. Kuhn and G. Rodrigo, Phys. Rev. **D59**, 054017 (1999), hep-ph/9807420.
- [31] G. L. Bayatian *et al.*, CMS Collaboration, J. Phys. **G34**, 995 (2007).
- [32] V. M. Abazov *et al.*, D0 Collaboration, Phys. Rev. Lett. **101**, 191801 (2008), arXiv:0804.3220.
- [33] D. E. Acosta *et al.*, CDF Collaboration, Phys. Rev. **D71**, 052002 (2005), hep-ex/0411059.
- [34] J. C. Collins and D. E. Soper, Phys. Rev. **D16**, 2219 (1977).
- [35] O. Antunano, J. H. Kuhn, and G. Rodrigo, Phys. Rev. **D77**, 014003 (2008), arXiv:0709.1652.
- [36] G. Rodrigo, Proc. Sci., **RADCOR2007**, 010 (2007), arXiv:0803.2992.
- [37] P. Ferrario and G. Rodrigo, Phys. Rev. **D78**, 094018 (2008), arXiv:0809.3354.
- [38] P. Ferrario and G. Rodrigo, Proc. Sci., DIS2010 (2010) 191, arXiv:1006.5593.
- [39] S. Lowette, J. Dhondt, J. Heyninck and P. Vanlaer, CMSNote 2006/013 2006.
- [40] LHCb Collaboration, Report No. CERN-LHCC-2001-011 LHCb TDR5, 2001.